Cryobiology 118 (2025) 105191

Contents lists available at ScienceDirect

Cryobiology

journal homepage: www.elsevier.com/locate/cryo

The role of microRNA in the regulation of hepatic metabolism and energy-expensive processes in the hibernating dormouse

W. Aline Ingelson-Filpula [a,*], Anna Kübber-Heiss [b], Johanna Painer [b], Gabrielle Stalder [b], Hanane Hadj-Moussa [c], Fabrice Bertile [d], Caroline Habold [e], Sylvain Giroud [b,**,1], Kenneth B. Storey [a,1]

[a] Institute of Biochemistry and Department of Biology, Carleton University, 1125 Colonel By Drive, Ottawa, Ontario, K1S 5B6, Canada
[b] Research Institute of Wildlife Ecology, Department of Interdisciplinary Life Sciences, University of Veterinary Medicine, Vienna, Austria
[c] The Babraham Institute, Babraham Hall House, Babraham, Cambridge, CB22 3AT, United Kingdom
[d] University of Strasbourg, CNRS, IPHC, UMR, 7178, Laboratoire de Spectrométrie de Masse Bio-Organique, Strasbourg, France
[e] University of Strasbourg, CNRS, IPHC, UMR, 7178, Ecology, Physiology & Ethology Department, Strasbourg, France

ARTICLE INFO

Keywords:
Body temperature
Torpor
Epigenetic regulation
Metabolic rate depression
Post-transcriptional regulation

ABSTRACT

The garden dormouse (*Eliomys quercinus*) is a fat-storing mammal that undergoes annual periods of hibernation to mitigate the effects of food scarcity, low ambient temperatures, and reduced photoperiod that characterize winter. Like other hibernating species, this animal suppresses its metabolic rate by downregulating nonessential genes and processes in order to prolong available energy stores and limit waste accumulation throughout the season. MicroRNAs (miRNAs) are short, single-stranded, noncoding RNAs that bind to mRNA and mediate post-transcriptional suppression, making miRNA ideal for modulating widespread changes in gene expression, including global downregulation typified by metabolic rate depression. Using next-generation sequencing, we analyzed an RNA-seq dataset to determine which miRNAs are differentially regulated during hibernation in the dormouse liver. We found that the expression of 19 miRNAs was altered during hibernation; however, only one major miRNA (miR-34a-5p) remained significantly downregulated after correcting for false discovery rate. Gene Ontology, KEGG Pathway Analysis, and DIANA-miRPath predicted that energy metabolism, nuclear-related functions such as histone binding, chromatin- and chromosomal binding, and the cell cycle are processes that may be differentially regulated during hibernation due to miRNA regulation. Taken together, our data suggest that miRNA influence appears to be strongly directed toward suppressing energy-intensive processes in the nucleus hence contributing to extend the animal's endogenous fuel reserves for the duration of hibernation.

1. Introduction

The garden dormouse (*Eliomys quercinus*) is a rodent endemic to Western Europe that uses circannual hibernation to avoid the deleterious environmental conditions characteristic of winter, including sub-zero temperature, reduced food availability, and short photoperiod. Hibernation is broadly classified as a series of torpor bouts – torpor itself being distinguished by a vast reduction in metabolic rate by ~95 % of euthermic levels and a concomitant decrease in mobility, cardiac and respirometry rates, and body temperature (T_b), which drops to near-ambient temperatures (T_a) [1,2,3]. Each torpor bout is interspersed with brief periods of euthermia, called interbout arousal, in which the animal raises its T_b back to ~37 °C via non-shivering and shivering thermogenesis, metabolic rate increases to pre-hibernation levels, and the animal carries out any necessary pro-survival functions and corrects metabolic imbalances before entering another torpor bout [1,4]. On the biochemical level, hibernation encompasses a suite of molecular adaptations which allows the animal to make drastic changes to its phenotype including the drop in metabolic, heart, and respirometry rates as well as the decrease in T_b [5].

To prepare for hibernation, *E. quercinus* enters a hyperphagic state by consuming large amounts of food in the fall to build up fat reserves,

* Corresponding author.
** Corresponding author.
E-mail addresses: alineingelsonfilpula@cmail.carleton.ca (W.A. Ingelson-Filpula), sylvain.giroud@vetmeduni.ac.at (S. Giroud).
[1] Contributed equally to the study.

https://doi.org/10.1016/j.cryobiol.2024.105191
Received 24 May 2024; Received in revised form 15 December 2024; Accepted 19 December 2024
Available online 1 January 2025

allowing it to survive solely on its endogenous fuel stores for the duration of hibernation. This classifies *E. quercinus* as a fat-storing hibernator, contrary to food-storing hibernators which include Syrian hamsters [2]. In *E. quercinus*, hibernation lasts approximately 5–6 months and can be subdivided into ~20 torpor bouts of 8 days each, interposed with interbout arousals lasting about 6 h [2,6]. Similar to other mammals that undergo torpor and/or hibernation as a winter survival strategy, *E. quercinus* employs metabolic rate depression (MRD) – the global downregulation of nonessential genes and processes and reprioritization of metabolic pathways – to mitigate these changes [5]. MRD is well-characterized in a variety of animal models ranging from mammals to invertebrates, which enter a hypometabolic state to survive their respective extreme environmental stresses [7]. Coordinating such large-scale suppression of cellular processes without leading to catastrophic downstream effects, and while avoiding physiological detriments upon hibernation exit, requires a myriad of biochemical factors operating at the DNA, RNA, and protein levels. The field of epigenetics and how it affects hibernation is vastly expanding [8,9], microRNAs (miRNA) and mRNA modifications are being investigated [10,11], and changes in protein expression or post-translational modifications to the proteins themselves are becoming elucidated [12].

MiRNAs are single-stranded, noncoding RNAs of 21–25 nt that control gene expression at the post-transcriptional level, through binding to mRNA transcripts for translational suppression [13]. Moreover, their synthesis is rapid, reversible, and energetically inexpensive. They are therefore ideal for implementing and maintaining hibernation and its high phenotypic plasticity. Binding of miRNAs to mRNAs occurs via an 8 nt seed sequence at the 5' end of the miRNA – perfect complementarity to the mRNA leads to degradation, while imperfect complementarity redirects the transcript to storage and thus suppresses translation [13]. MiRNAs have already been implicated during hibernation in a variety of species and tissues, making them ideal candidates to investigate in *E. quercinus* [10,11,14,15,16].

Next-generation sequencing is a potent tool, which allows screening for all small RNA species in a particular tissue/set of conditions, which can be further processed to detect miRNAs that may be differentially regulated during hibernation [17,18]. Downstream effects of these miRNAs can be predicted using bioinformatic tools and analyses [19]. Therefore, this study uses next-generation sequencing to study the *E. quercinus* liver "miRNAome", comparing summer-active and torpid dormice. The liver is the most metabolically active organ, facilitating the balance of lipids and sterols in the plasma and gut and being largely responsible for metabolic homeostasis; we thus anticipated a high likelihood of miRNA involvement in these processes [20,21]. The miRNAs that are differentially regulated during hibernation were detected, and Gene Ontology and Kyoto Encyclopedia of Genes and Genomes pathway mapping was used to predict the downstream effects of differentially-regulated miRNAs. DIANA-miRPath was used to predict individual gene targets in these downstream processes. Overall, this research will increase our understanding of hibernation in another fat-storing hibernator, allowing us to gain valuable insights into how mammalian species implement hibernation as a whole, whether through conserved or species-specific strategies.

2. Materials and methods

2.1. Animal collection and treatment

The adult garden dormice used in this study were bred and raised at the Research Institute of Wildlife Ecology (FIWI), Vienna, Austria (latitude 48°15′N, longitude 16°22′E). Animals were held in outdoor enclosures under natural photoperiod and T_a. Prior to hibernation, dormice were housed separately in polycarbonate cages (60 × 40 × 40 cm) and had access to water and food *ad libitum* (Altromin 7024, Altromin GmbH & Co. KG, Lage, Germany). Additional nutrition was provided two times per week (sunflower seeds and dry insects). Once dormice attained a plateau for body mass and food intake was largely reduced, the animals were determined ready to enter prolonged torpor or hibernation [22,6]. The experiments involved eight garden dormice (three males, five females) with a mean body mass of 135.8 ± 16.8 g [CI 115.6–161.4 g] prior to hibernation.

2.2. Animal protocol overview

Hibernation was induced by housing the animals at 4 °C without food and water, to mimic conditions of winter hibernation as previously described [23]. During the three months of the experiment, core T_b via temperature transmitters was measured continuously in torpid dormice (read section below for more details about T_b measurements). Animals, with a mean body mass of 108.5 ± 12.7 g [CI 92.1–130.9 g], were sacrificed at mid-winter (December to January) when torpor bout lengths are maximal, either in torpor or during interbout euthermia, by immediate decapitation (if torpid; T_b: 4.70 ± 0.34 °C measured via implanted transmitters) or by CO_2-euthanasia followed by decapitation as previously described in Ref. [23] (if euthermic, T_b: 37.22 ± 0.12 °C measured via implanted transmitters). A representative schematic of the animal experiment workflow can be found in Supplementary Fig. 1. Tissues were quickly sampled and immediately flash frozen in liquid nitrogen (−196 °C) and stored at −80 °C for 4–12 months until shipped to Carleton University on dry ice for subsequent analyses.

2.3. Surgical implantation of transmitters and body temperature measurements

Prior to hibernation, animals were implanted with small temperature transmitters and core T_b was monitored via a telemetry system. TA-F10 transmitters (1.1 cc, 1.6g, accuracy: 0.15 °C; Data Sciences International, St Paul, US) were calibrated prior to implantation between 0 and 40 °C in a temperature-controlled water bath. Surgery proceeded as previously described [24]. In short, transmitters were surgically implanted under anesthesia induced by subcutaneous injection of 50 mg kg^{-1} ketamine (Ketamidor® 10 %, Richter Pharma, Wels, Austria) and 5 mg kg^{-1} xylazine (Rompun® 2 %, Bayer, Leverkusen, Germany), and maintained using 1.5 % isoflurane via facemask. A subcutaneous administration of 5 mg kg^{-1} ketoprofen (Romefen® 10 %, Merial S.A.S., Toulouse, France) was provided as post-operative analgesic. Following surgery, animals recovered for ten days before temperature recordings were started. An RPC-1 receiver board (Data Sciences International) was positioned under each individual cage to collect transmitter data. A 10s T_b measurement was recorded every 5 min, and data was analyzed using the Dataquest software (LabPro Data Sciences).

2.4. RNA extraction

RNA was extracted from liver tissue of euthermic and torpid *E. quercinus* (n = 4 for both conditions). Flash-frozen tissue weighing ~50 mg was crushed under liquid nitrogen and homogenized in 1 mL of TRIzol reagent (Invitrogen; Cat. # 15596-018). 200 μL of chloroform was added, and samples were centrifuged at 10,000×g for 15 min at 4 °C. The upper RNA-containing aqueous phase was transferred to a sterile microcentrifuge tube with 500 μL of 2-propanol. Tubes were incubated for 10 min at room temperature to precipitate out RNA, and centrifuged at 10,000×g for 15 min at 4 °C to form an RNA pellet. Pellets were washed 2 × with 70 % ethanol and air-dried for 10–15 min, before resuspending with 50 μL of RNAse-free water. Concentration/purity of total RNA was determined with an OD 260/280 ratio of ~2.0 using a BioTek Take3 microspot plate and a PowerWave HT microplate spectrophotometer. RNA integrity was confirmed with agarose gel (1 %) electrophoresis.

2.5. Small RNA sequencing

RNA samples from the liver of euthermic vs. torpid *E. quercinus* were sequenced by BC Cancer Agency (Vancouver, BC, Canada). RNA quality was confirmed using an Agilent Bioanalyzer 2100 system (Agilent Technologies, Santa Clara, CA, USA) prior to miRNA library construction. Small RNA cDNA libraries were assembled as detailed in Ref. [25], validated with the Bioanalyzer, and sequenced with an Illumina HiSeq 2500 platform.

2.6. Read processing

Small-RNA raw data files from BC Cancer Agency were uploaded to the SRA database and are available at SRA Accession: PRJNA955229. Raw read data was processed as described in Ref. [26]. Cutadapt was used to filter out low-quality reads and remove the 6-nucleotide adapters [27]. FastQC was used to validate both successful adapter removal and proper distribution of small RNA lengths to ~25 nt [28]. To isolate only mature miRNA sequences from other non-miRNA small RNAs (tRNA, rRNA, piRNA, snRNA, and snoRNA), reads were aligned to a negative reference file (compiled from Rfam [29] and piRNABank databases [30]) and eliminated using bowtie [31]. Remaining reads were screened for mature miRNAs using bowtie, drawing from mature miRNA sequences from miRBase, the miRNA database [32], as a positive reference file with the parameters of perfect seed sequence matches and a seed sequence length of 20 nt. The reads that aligned to mature miRNA sequences were sorted, and read counts were determined for each miRNA using samtools [33] and Unix command line tools. MiRNAs with less than four reads were eliminated, and read counts were normalized as detailed in Ref. [26] using the voom method [34].

2.7. Differential expression analysis and clustering

Differential expression of miRNAs between euthermic and torpid animals was determined the limma R package [35], which uses linear model fitting with empirical Bayesian testing. Differentially expressed miRNAs were considered significant with 1) false discovery rate (FDR)-corrected p-value <0.05, and 2) absolute $\log_2$ fold-change ≥ 1.5. False discovery rate is used for large-scale omics studies which test many hypotheses and wish to minimize the frequency of false positives among all the rejected hypotheses [36]. This statistical correction makes use of the t-distribution for the T-statistic rather than a normal approximation [36,37].

2.8. Gene set analysis

The RBiomirGS R package [19] was used to conduct gene set analysis to determine both significantly enriched gene ontology (GO) terms [38] and Kyoto Encyclopedia of Genes and Genomes (KEGG) pathways [39]. This package uses multiple databases to enumerate miRNA:mRNA interactions, and calculates both a miRNA score ($S_{microRNA}$) and a mRNA score (S_{mRNA}) to quantify the number of potential interactions between different miRNAs and the particular mRNA targets [40].

RBiomirGS uses the calculated S_{mRNA} of mRNAs to identify significantly enriched gene sets (FDR-adjusted p-value ≥ 0.05) and corresponding model coefficients for each GO term and KEGG pathway. A negative model coefficient signifies the GO term/KEGG pathway is downregulated due to increased negative regulation by miRNA, and vice versa a positive model coefficient indicates that regulation by miRNA is decreased and may promote the pathway during hibernation as compared to euthermia. Estimated model coefficients and standard error are calculated by a logistic regression-based method, which are then applied to determine statistical significance [19].

2.9. DIANA-miRPath prediction of miRNA targets

To characterize miRNA target prediction, mature miRNA sequences from *Homo sapiens* were searched for potential gene pairings in hallmark gene sets using DIANA-miRPath (v.4.0). DIANA-miRPath was used with the following parameters: direct targeting from TarBase v8.0 [41]; miRNA annotation from miRbase-v22.1; genes union merging method; and classic analysis testing method. DIANA-miRPath generated a list of hallmark gene sets containing miRNA-targeted genes which were functionally enriched and analyzed using an FDR-corrected p-value <0.05. Given that only one miRNA was statistically significant with FDR correction, pathway enrichment analysis for miRNA-targeted clusters was expanded to include the 19 miRNAs with noncorrected p-values <0.05. This analysis was performed using the Molecular Signatures Database (MSigDB) available for *H. sapiens* [42]. Results were downloaded in.csv format and visualized using R (version 4.4.1) and RStudio with packages ggplot2 [43], RColorBrewer [44], tidyr [45], and dplyr [46].

2.10. Statistical analysis and visualization

Volcano plots, heatmaps, and biplots for differential expression and gene set analysis were produced using either matplotlib and seaborn python packages, or Microsoft Excel [47,48]. Hierarchical clustering of significantly differentially regulated miRNAs was produced by the gplots R package [49].

3. Results

3.1. 148 mature miRNAs were detected in liver

The mean number of raw reads from a $n = 4$ of euthermic vs. torpid liver, respectively, was 22,280,371 ± 1,542,776 and 24,325,682 ± 881,993. After negative filtering, 8,392,637 ± 471,888 reads in the euthermic group and 9,604,694 ± 877,402 reads in the torpid group aligned to 148 mature miRNA sequences. Raw genome files are available at SRA Accession: PRJNA955229.

3.2. One FDR-corrected miRNA (miR-34a-5p) but 19 non-FDR-adjusted miRNAs were differentially-expressed during torpor

Of the 148 miRNAs that matched with a mature sequence from miRBase, only one miRNA (hsa-miR-34a-5p) was statistically significant after adjusting for false discovery rate (FDR), and displayed a 1.72-fold downregulation during torpor compared to euthermia (Supplementary Table 1; Fig. 1). When examining mature miRNAs without FDR correction and a p-value of <0.05, 19 miRNAs would have been differentially regulated. Of these, 7 have negative model coefficients (demonstrating downregulation of the respective miRNA), and 13 have positive model coefficients, indicating potential upregulation (Supplementary Table 1). Given the necessary rigor of FDR correction in multi-omic studies, the FDR-corrected results are visualized using a volcano plot with red markers corresponding to the significantly downregulated miRNA (Fig. 1; Supplementary Table 1).

3.3. Enriched gene ontology terms included chromatin and RNA processes influenced by miR-34a-5p

GO terms from the three GO domains (Biological Processes, Cellular Compartment, and Molecular Function) were all used to predict miRNA influence. All GO results are visualized using volcano plots with red markers corresponding to the terms with negative model coefficients, and blue markers for positive model coefficients. Full data for each GO analysis can be found in Supplementary Tables 2–4.

GO Biological Processes had 103 statistically significant FDR-adjusted terms. Of these, 72 displayed positive model coefficients,

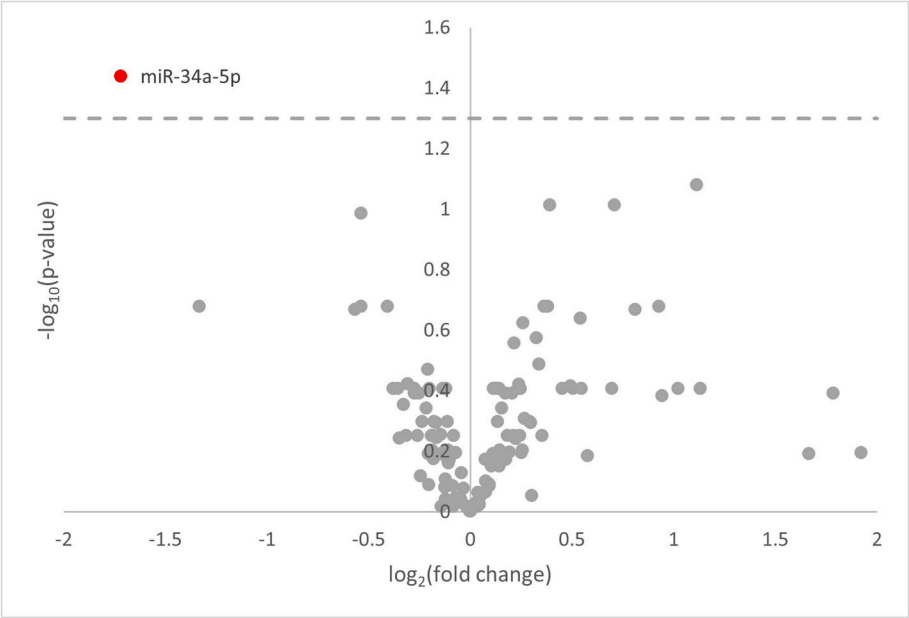

Fig. 1. Differentially-expressed miRNA in euthermic vs. torpid *E. quercinus* liver. Data displayed in a volcano plot with fold-change thresholds set to $\pm \log_2 1.5$ and a false discovery rate (FDR)-adjusted *p*-value <0.05. Red markers indicate significantly downregulated miRNA. Grey circles are miRNA that did not pass the fold-change and p-value thresholds. (For interpretation of the references to colour in this figure legend, the reader is referred to the Web version of this article.)

signifying upregulation of the respective term via miRNA in the liver of torpid dormice (Fig. 2; Supplementary Table 2). Likewise, the 31 remaining terms had negative model coefficients, suggesting down-regulation of these processes during hibernation. The top five GO Biological Process terms are GO Chromatin Silencing at rDNA, GO Protein Heterotetramerization, GO Chromatin Silencing, GO Chromatin Assembly or Disassembly, and GO Negative Regulation of Gene Expression.

GO Cellular Compartment had 17 statistically significant terms when adjusted for FDR (Fig. 3; Supplementary Table 3). Of these, 3 had negative model coefficients (GO Nuclear Membrane Part, GO Lytic Vacuole, and GO Pre-Autophagosomal Structure), while 15 displayed positive model coefficients.

Twelve GO Molecular Function terms were differentially regulated in the torpid liver, with 2 negative model coefficients (GO Translation Elongation Factor Activity and GO Calmodulin Dependent Protein Kinase Activity) and 10 positive model coefficients, many of them related

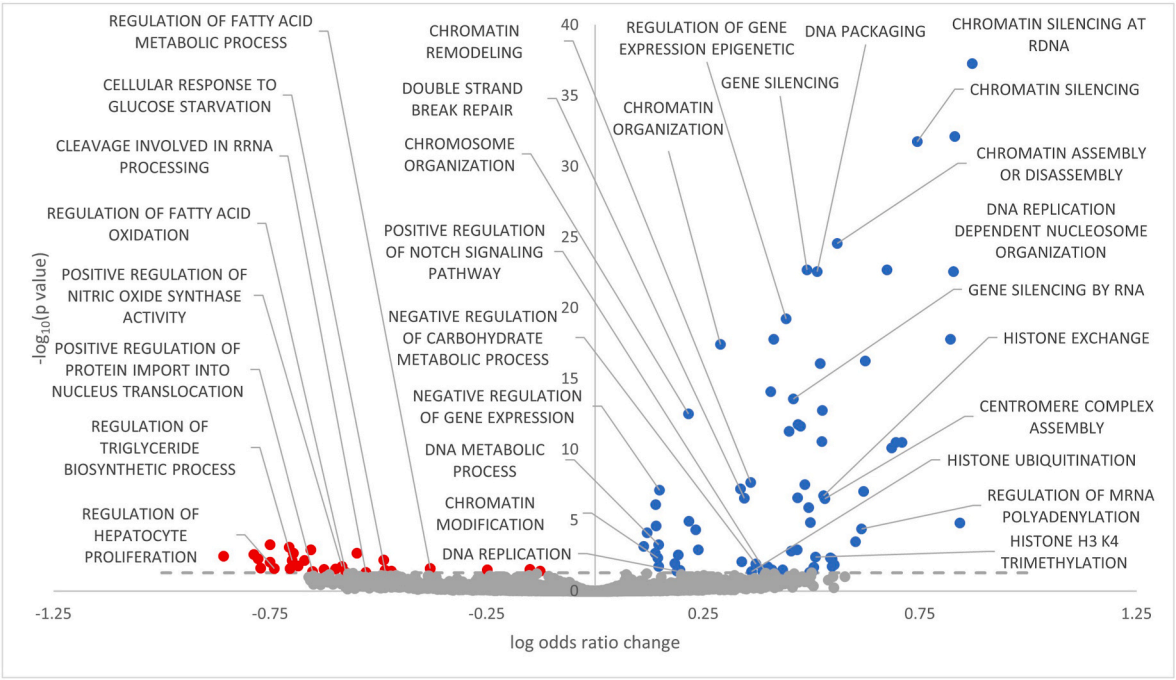

Fig. 2. GO Biological Processes affected by differential miRNA expression in euthermic vs. torpid *E. quercinus* liver. All terms are enriched with an FDR-adjusted *p*-value <0.05. Red and blue markers indicate statistically-significant terms with negative and positive model coefficients, respectively. A negative coefficient indicates upregulation of miRNA targeting the genes encompassed in that term (thus potentially downregulating the genes), and vice versa for positive coefficient. (For interpretation of the references to colour in this figure legend, the reader is referred to the Web version of this article.)

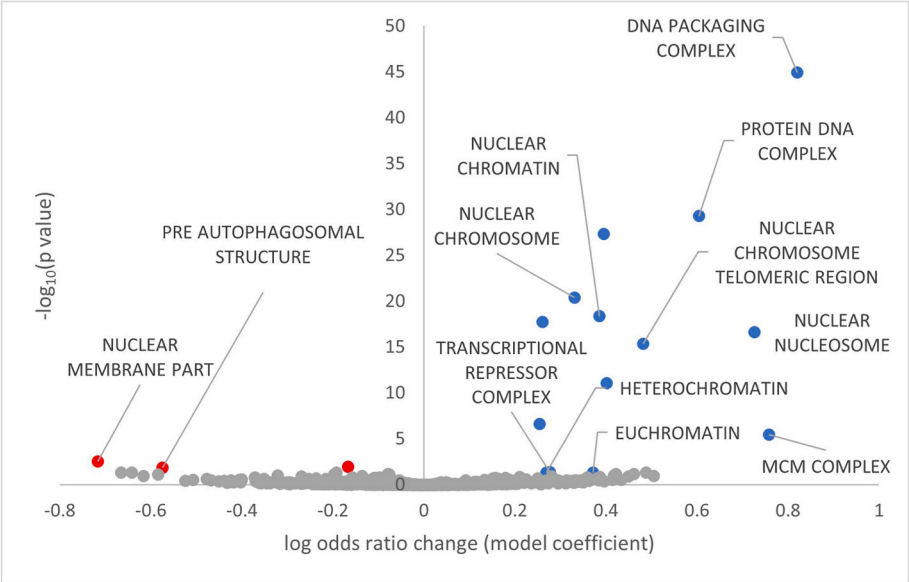

Fig. 3. GO Cellular Compartment enriched by differentially expressed miRNA in euthermic vs. torpid *E. quercinus* liver. Red and blue markers indicate statistically-significant terms with negative and positive model coefficients, respectively. A negative coefficient indicates upregulation of miRNA targeting the genes encompassed in that term (thus potentially downregulating the genes), and vice versa for positive coefficient. All terms are enriched with an FDR-adjusted *p*-value <0.05. (For interpretation of the references to colour in this figure legend, the reader is referred to the Web version of this article.)

to chromatin and RNA processes ($p < 0.05$; Fig. 4; Supplementary Table 4). For example, the top five GO Molecular Function terms when sorted by smallest FDR-adjusted *p*-value are GO Histone Binding, GO Protein Heterodimerization Activity, GO Protein Dimerization Activity, Go Nucleosome Binding, and GO Nucleosome DNA Binding ($p < 0.05$; Fig. 4).

3.4. KEGG pathways with differential miRNA regulation included insulin signaling and cell cycle

KEGG pathway analysis identified 6 pathways with predicted differential regulation during hibernation ($p < 0.05$; Fig. 5; Supplementary Fig. 5). GO Insulin Signaling Pathway had a negative model coefficient and an FDR-adjusted *p*-value of 0.015. Meanwhile, GO DNA Replication and GO Cell Cycle had positive model coefficients and $p = 0.0056$. KEGG results are visualized using a volcano plot with red markers corresponding to significantly downregulated miRNAs and blue markers corresponding to significantly upregulated miRNAs (Fig. 5, Supplementary Table 5).

3.5. DIANA-miRPath predictions of miRNA gene targets

Using miRNA–gene target predictions from TarBase, the following hallmark gene sets with their respective miRNA-targeted genes were

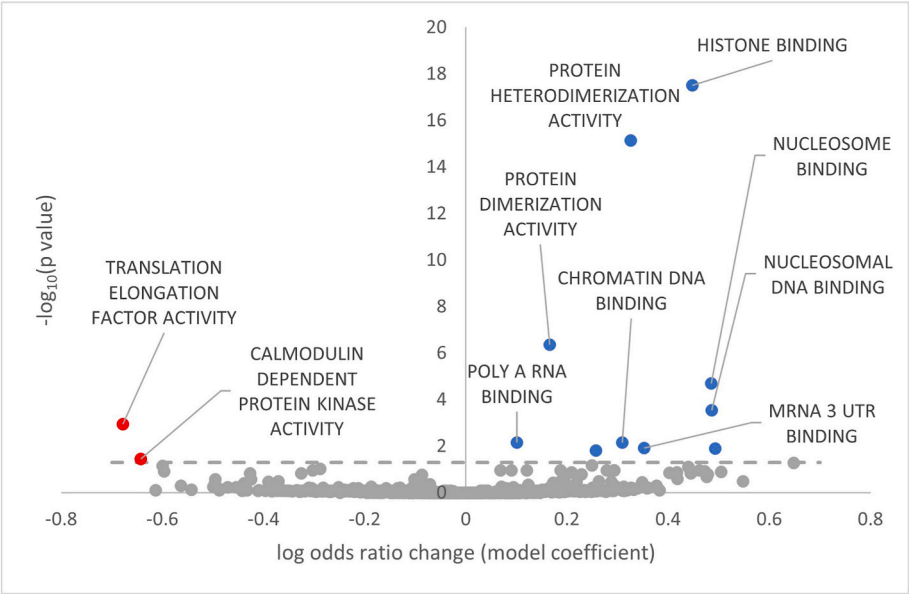

Fig. 4. GO Molecular Function enriched by differential miRNA expression in euthermic vs. torpid *E. quercinus* liver. Red and blue circles indicate statistically-significant terms with negative and positive model coefficients, respectively. A negative coefficient indicates upregulation of miRNA targeting the genes encompassed in that term (thus potentially downregulating the genes), and vice versa for positive coefficient. All terms are enriched with an FDR-adjusted *p*-value <0.05. (For interpretation of the references to colour in this figure legend, the reader is referred to the Web version of this article.)

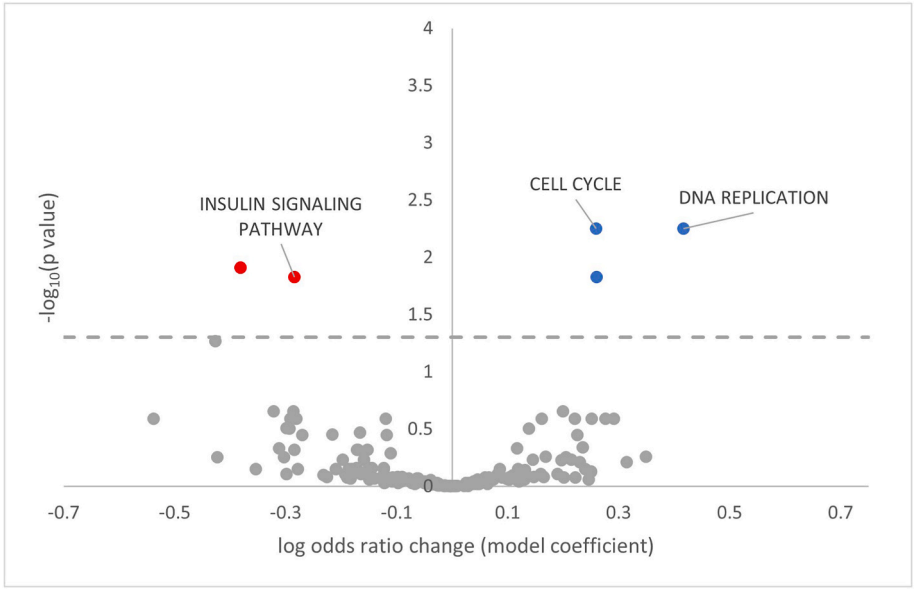

Fig. 5. KEGG Pathway Analysis of differentially expressed miRNA in euthermic vs. torpid *E. quercinus* liver. Red and blue markers indicate statistically-significant terms with negative and positive model coefficients, respectively. A negative coefficient indicates upregulation of miRNA targeting the genes encompassed in that term (thus potentially downregulating the genes), and vice versa for positive coefficient. All terms are enriched with an FDR-adjusted *p*-value <0.05. (For interpretation of the references to colour in this figure legend, the reader is referred to the Web version of this article.)

identified. The statistically-significant hallmark gene sets included: (1) G_2M checkpoint; (2) UV response; (3) mTORC1 signaling; (4) E2F targets; (5) MYC targets; (6) mitotic spindle; (7) protein secretion; (8) TGFβ signaling; (9) unfolded protein response; (10) androgen response; (11) TNFα signaling via NFκB; (12) hypoxia; (13) p53 pathway; (14) epithelial-mesenchymal transition; (15) early estrogen response; (16) apoptosis; (17) adipogenesis; and (18) glycolysis. These results are visualized in Fig. 6A and reported in Supplementary Table 6. The specific miRNA-targeted genes from individual hallmark gene sets were extracted (totalling 1428 unique genes) and visualized against (1) the number of hallmark gene sets the gene was present in, and (2) the number of unique miRNAs which targeted the gene (Fig. 6B; Supplementary Table 7).

4. Discussion

This study used next-generation sequencing to analyze an RNA-seq dataset from euthermic vs. torpid *E. quercinus* liver. Bioinformatic analysis predicted that one miRNA was downregulated during hibernation (when FDR-adjusted), with the possibility for 19 other ones without this adjustment. Gene Ontology is a method of network mapping for gene expression, which groups gene targets into their 1) biological processes, 2) cellular compartment they act within, and 3) molecular functions [38]. GO Biological Processes, GO Cellular Compartment, GO Molecular Function, and KEGG pathway analysis were used to predict cellular roles influenced by miRNAs during hibernation, and specific gene targets were predicted with DIANA-miRPath.

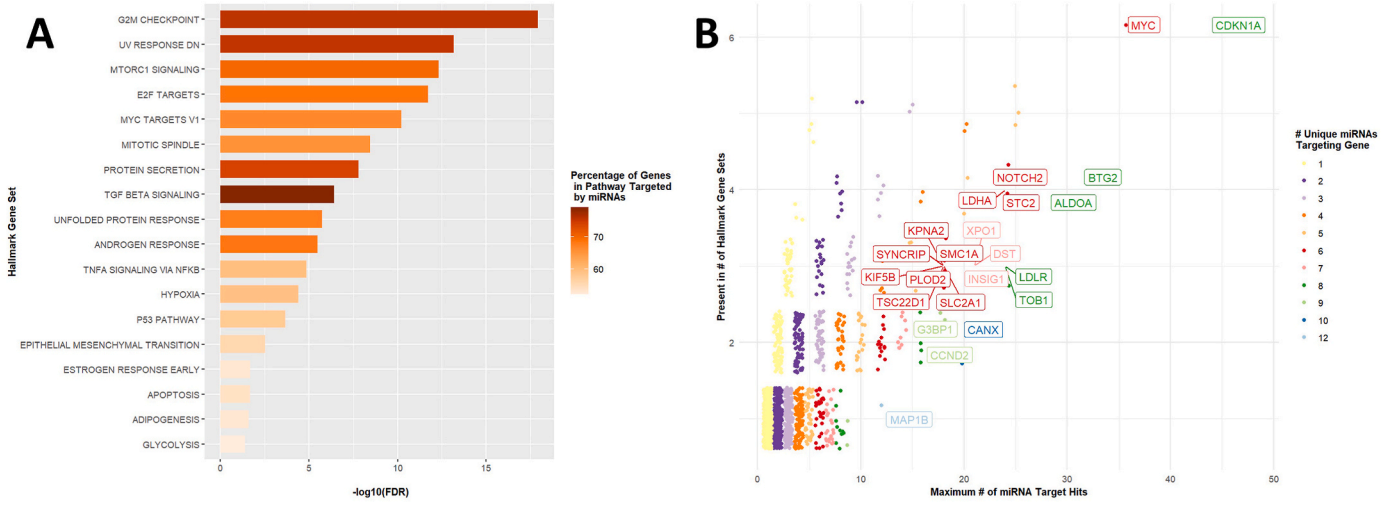

Fig. 6. DIANA-miRPath hallmark gene sets (A) and genes union predictions (B) for differentially expressed miRNA in euthermic vs. torpid *E. quercinus* liver. MSigDB and TarBase v8.0 were used for target predictions. Color in (A) refers to the percentage of genes in the total gene set targeted by at least one differentially-expressed miRNA. Genes in (B) are arranged by the and overall count of unique miRNA-gene targets across all gene sets, and the number of unique hallmark gene sets they are present in. Color refers to the number of unique differentially-expressed miRNAs which target that gene. All terms are enriched with an FDR-adjusted *p*-value <0.05. (For interpretation of the references to colour in this figure legend, the reader is referred to the Web version of this article.)

4.1. Processes in line with metabolic rate depression

In a broad sense, many of the molecular changes that occur during hibernation contribute to maintaining MRD – the suppression of nonessential and energy-intensive genes and processes in order to optimize the use of the animal's endogenous fuel reserves for the duration of hibernation. Indeed, we see evidence of this in the differentially-regulated GO terms, especially GO Biological Processes. There is a downregulation (i.e., terms with negative model coefficients) of GO Regulation of Hepatocyte Proliferation and GO Regulation of Triglyceride Biosynthetic Process, suggesting that energy-intensive proliferation is suppressed during hibernation ($p < 0.05$; Fig. 2). Likewise, Negative Regulation of Gene Expression, Negative Regulation of Carbohydrate Metabolic Process, Gene Silencing, and Gene Silencing by RNA all displayed positive model coefficients ($p < 0.05$; Fig. 2). More succinctly, there is an increase in negative regulation of gene expression during hibernation, which falls perfectly in line with overarching themes of MRD.

There may be differential regulation of Notch signaling during hibernation, as evidenced by the statistically significant GO term Positive Regulation of Notch Signaling Pathway which is upregulated in GO Biological Processes ($p < 0.05$; Fig. 2). DIANA-miRPath predicted 6 miRNAs (let-7i-5p; miR-15b-5p; miR-181b-5p; miR-25-3p; miR-29b-1-5p; and miR-34a-5p) which target NOTCH2 (Fig. 6B; Supplementary Table 7). Notch signaling is an evolutionary conserved pathway in most multicellular animals, and its functions can span both transcriptional activation and transcriptional repression based on its co-activators [50]. Potential outcomes of Notch signaling include entering the MAPK cascade via Ras, with further downstream pathways of p53, cell cycle, apoptosis, Wnt, and gene expression [51,52,50], all of which are modulated during hibernation [53,54,55,56,57]. Indeed, these pathways were also represented by DIANA-miRPath, with p53 signaling, apoptosis, and cell cycle-related gene sets (G_2M checkpoint and mitotic spindle) having more than 60 % of their genes as predicted targets for the torpor-induced differentially expressed miRNAs ($p < 0.05$; Fig. 6A; Supplementary Tables 6 and 7). While precise levels of cofactors and Notch itself would need to be measured in order to determine the functional downstream effects of Notch signaling, it is interesting that transcriptional repression via Notch can be enacted through histone modification enzymes [58]. Specifically, histone H3K4 is dynamically methylated at transcription factor RBP-J, which is critical for Notch activation [58]. The GO Biological Processes term Histone H3K4 Trimethylation is statistically significant with a positive model coefficient, along with a myriad of other histone-related GO terms which will be addressed later in this discussion ($p < 0.05$; Fig. 2). However, it is possible that Notch signaling serving transcriptional repression-related purposes could be contributing to MRD in torpid *E. quercinus* liver.

Downstream effects of Notch signaling remain active throughout organismal development, and encompass apoptosis, cellular proliferation/differentiation, and pro-survival functions [51]. Dysregulated Notch signaling in liver can induce liver fibrosis through mobilization of hepatic stellate cells, whereas other factors of the Notch pathway mitigate liver inflammation, regeneration, and fibrogenic repair [59]. Therefore, differential regulation of Notch signaling during hibernation may have an additional role in modulating liver damage responses, whether through anti-apoptotic or pro-survival means.

4.2. Hibernation induces changes in energy metabolism

When adjusting for false discovery rate (FDR), only one but major miRNA was predicted to be differentially-regulated – miR-34a-5p (Fig. 1; Supplementary Table 1). This miRNA is linked with energy metabolism; for example, overexpression of miR-34a-5p promotes glucose production in hepatocytes through inhibiting SIRT1 [60]. Hepatic gluconeogenesis is tightly controlled with glucagon- and insulin signaling pathways, and varies between hibernating species. In *Ictidomys tridecemlineatus*, hepatic gluconeogenesis during hibernation is lowered; whereas in arctic ground squirrels and golden-mantled ground squirrels, hepatic gluconeogenesis appears to upregulate during hibernation [61,62,63]. In our study, GO Insulin Signaling Pathway was downregulated during hibernation in KEGG pathway analysis ($p < 0.05$; Fig. 5). This suggests that a decrease in miR-34a-5p as seen in Fig. 1 would lead to downstream effects of decreased glucose production during hibernation. This is supported by positive regulation of the GO Biological Process term Negative Regulation of Carbohydrate Metabolic Process. Meanwhile, GO Cellular Response to Glucose Starvation, GO Regulation of Fatty Acid Oxidation, and GO Regulation of Fatty Acid Metabolism were all statistically significant with negative model coefficients ($p < 0.05$; Fig. 2). Additionally, miR-34a-5p was predicted to target 24 genes in the adipogenesis hallmark gene set and 26 genes in the glycolysis hallmark gene set as per DIANA-miRPath, with the sum total of all miRNA-gene pairings encompassing ~50 % of the genes in both gene sets (Fig. 6; Supplementary Tables 6 and 7). The fatty acid terms having negative model coefficients might point to decreased *regulation* of these pathways, resulting in "unfettered" fatty acid metabolism which serves a critical role during hibernation, as opposed traditional regulation of these pathways during euthermia.

The liver also facilitates sterol-lipid equilibrium, since excess cholesterol is stored rather than excreted during hibernation [21]. Other fat-storing hibernators including *I. tridecemlineatus* have marked changes in insulin-related pathways which allow them to become a sort of natural model for reversible insulin resistance [64]. MiRNAs which target key players of metabolic and signaling cascades have been documented in *I. tridecemlineatus* liver, heart, and skeletal muscle [65]. Furthermore, in brown fat of hibernating *I. tridecemlineatus*, miRNA analysis revealed glycolysis/gluconeogenic pathways as being downregulated during hibernation, reinforcing the switch to fatty acid oxidation as the primary means of fuel consumption [14].

Nonetheless, these responses do not quite correlate with existing knowledge of altered fuel usage during hibernation. *E. quercinus* is a fat-storing hibernator which relies on fatty acid oxidation and gluconeogenesis for the duration of hibernation [2]. While fatty acid metabolism appears to have decreased regulation given the concurrent decrease in miR-34a-5p, the additional downregulation of carbohydrate metabolic pathways when gluconeogenesis activation is a robustly-observed phenomenon in fat-storing hibernators is perplexing. While studies on specifically *E. quercinus* metabolism during hibernation have not been deeply researched, plasma profiles as well as transcriptomic and proteomic studies in *I. tridecemlineatus* during hibernation strongly support 1) decrease of triglycerides and increase of ketone bodies, 2) fatty acid oxidation; and 3) activation of gluconeogenesis to maintain glycemia [66,67,68,69,70]. Liver transcriptomics in other hibernators corroborate these themes; for example, in the hibernating Syrian hamster *Mesocricetus auratus*, there were GO terms encompassing response to lipid, cellular response to hormone/insulin stimulus, and KEGG pathway analysis suggesting insulin resistance as well [71]. Differential regulation of metabolic-related genes including glucose-6-phosphate, glycogen phosphorylase, and pyruvate dehydrogenase served to inhibit glycolysis and oxidative phosphorylation, supporting the shift to fatty acid oxidation [71]. A similar pattern was denoted in *D. gliroides* liver, with the greatest changes in gene expression during torpor related to carbohydrate-lipid fuel switching, with four genes involved in promoting fat catabolism among the top five differentially expressed genes (upregulation of PDP2 and CYB5R3, downregulation of NR1H4 and ND4) [72]. *D. gliorides* liver also displayed a strong upregulation in TXNIP, which along with its antioxidant capacities is also involved in inhibiting unnecessary glucose influx into cells while also promoting fatty acid oxidation [73]. In hibernating *I. tridecemlineatus* liver, differentially-expressed genes during torpor were enriched for glucose and triglyceride metabolic processes, lysosome and polygenic dyslipidemia, urea cycle, nicotinamide metabolic processes, vitamin B6 binding, and heat shock proteins (HSPs) [74]. There appears to be an

overarching priority of increased fatty acid oxidation and modulation of carbohydrate-lipid metabolism genes, which may be reflected in our results by "unfettered" regulation of fatty acid metabolism. While it is possible that epigenetic, post-transcriptional, and/or post-translational modifications alter the final endpoint of metabolic pathways, further research will need to be done on miRNA influence on specific aspects of dormouse metabolism during hibernation, e.g., ketone bodies and gluconeogenesis.

4.3. Chromatin and RNA related processes

GO Cellular Compartment displayed a strong upregulation in many chromatin- and RNA related processes, including Nuclear Chromatin, Nuclear Chromosome, Hetero- and Euchromatin, Nuclear Chromosome Telomeric Region. Interestingly, quite a few GO terms point towards DNA replication and its associated constituents being upregulated via miRNA during hibernation. For example, KEGG had both Cell Cycle and DNA Replication with positive model coefficients, while GO Cellular Compartment has an upregulation of MCM Complex, DNA Packaging Complex, and Protein-DNA Complex ($p < 0.05$, Fig. 3). Finally, GO Biological Processes highlights terms including DNA Replication, Chromosome Organization, DNA Packaging, Chromatin Assembly or Disassembly, DNA Replication-Dependent Nucleosome Organization, and Centromere Complex Assembly ($p < 0.05$; Fig. 2). This is contrary to the established literature regarding the cell cycle during hibernation – protein levels of cell cycle machinery are overwhelmingly downregulated during hibernation in multiple species and tissues via multiple regulatory factors/processes [75,57]. The cell cycle is an energetically-expensive process, therefore the governing theme of MRD and a hypometabolic state indicates that the cell cycle is suppressed during hibernation [75]. The implication that the cell cycle is upregulated during hibernation is perplexing. However, there are alternate hypotheses we can propose for this phenomenon.

DIANA-miRPath included G_2M checkpoint and mitotic spindle as two cell cycle-related hallmark gene sets predicted to be disproportionally regulated by our differentially-regulated miRNA subset (affecting >75 % and >60 % of the genes in the pathways, respectively) (Fig. 6A; Supplementary Table 6). However, the genes in these two pathways are not exclusive, and may have a variety of functional roles elsewhere. For example, NOTCH2 was heavily represented in G_2M checkpoint despite its various other downstream roles, and cell-cycle specific proteins including CDKN1A were represented in multiple hallmark gene sets (6, in the example of CDKN1A) (Fig. 6; Supplementary Tables 6 and 7). The level of crosstalk and functional downstreams of genes targeted by these miRNAs could result in an "artificial" inflation of cell cycle-related terms, even if the individual genes are implicated in other processes.

Additionally, hibernation is not a continuous state of torpor – it is broken up into physiologically distinct stages (entrance, early torpor as first half of a torpor bout, late torpor being the latter half of a torpor bout, and interbout arousal) for the duration of the season [1]. During torpor, T_b rests at near-ambient temperatures, but during interbout arousal, T_b rises back to 37 °C via non-shivering followed by shivering thermogenesis so the animal can carry out any critical processes for the approximately 1-day length of the arousal [1]. For example, long-term fasting results in the small intestine losing mass and directing metabolism towards ketone body generation and fatty acid oxidation [76]. Interbout arousal periods may promote the cell cycle to stabilize intestinal mass and prevent extensive degradation of intestinal epithelium. The liver is additionally the most metabolically active organ, further reinforcing a potential need for cellular proliferation (which may involve Notch, as discussed previously) during these short windows of available cellular activity [2,20]. Another important note is that the animals in this study were sampled during late torpor; however, there is no known mechanism to determine how far away the animals were from an interbout arousal period. It is possible that the upregulation in cell cycle related processes corresponds to the anticipation of an impending interbout arousal period, for any necessary instance of cell division.

An alternative hypothesis is to examine MRD and hibernation more holistically than this study allows. We only examined miRNAs and their respective post-transcriptional regulatory capabilities, and all the GO and KEGG terms are predicated solely on miRNA and their effect during hibernation. However, this is not the entire picture during hibernation as a whole. MRD is coordinated by a vast interplay of regulatory factors, including epigenetic, post-transcriptional, and post-translational modifications [77,5]. It is therefore possible that while purely the *isolated* miRNA component might upregulate members of cell cycle machinery, other regulators in the cellular environment as a whole might counteract these effects. In the torpid liver of *I. tridecemlineatus*, Rb and SUV39H1 proteins were upregulated, indicating a strong regulatory "stop" of the G_1/S phase transition and corroborating results which show downregulation of cyclin and CDK complexes during hibernation [78,57]. Post-translational modifications of Rb which would convert it from an active to inactive form were notably absent during hibernation, highlighting the potent ability of post-translational roles in cell cycle suppression [78]. The cell cycle is also subject to a variety of epigenetic modifications which can cause acceleration or arrest of its various stages [79,80]. Although no dedicated studies have been conducted on epigenetic regulation and its effect on the cell cycle during hibernation, it is reasonable to assume that there are epigenetic controls for this process similar to what has been demonstrated in other tissues and other animal models of MRD [9,81,82]. Therefore, it is possible that the miRNA effects predicted in this study are counteracted by other existing epigenetic, post-transcriptional, and/or post-translational modifications. Indeed, this is already suggested by an upregulation in statistically significant GO terms involving mRNA polyadenylation and histone modification ($p < 0.05$; Fig. 2). Given that one miRNA can affect multiple mRNAs, and vice versa one mRNA can be targeted by a variety of miRNAs, this is in line with the fact that miRNAs influence in the torpid dormouse liver is directed toward other GO and KEGG terms, including those involved in energy metabolism or histone modifications that will now be discussed.

4.4. Histone binding and downstream effects

Histones are small positively-charged proteins that make up the nucleosome, the functional unit of chromatin. Histones are subject to many post-translational modifications including acetylation, methylation, and SUMOlyation of various amino acids that can lead to "tightness" or "relaxation" of chromatin, leading to varying levels of accessibility for the transcriptional machinery [83,84]. Chromatin remodeling is a characteristic effect of histone modification, involving dynamic interconversion between transcriptionally permissive euchromatin and repressive heterochromatin [85].

Many statistically significant GO terms from all three bioinformatics analyses involved histone modifications ($p < 0.05$; Figs. 2–4). These include Histone Exchange, Histone Ubiquitination, and Histone H3K4 Trimethylation from GO Biological Processes, Heterochromatin and Euchromatin from GO Cellular Compartment, and Histone Binding from GO Molecular Function ($p < 0.05$; Figs. 2–4). Trimethylation of H3K4, more commonly represented in the literature as H3K4me3, is incredibly conserved across species as being associated with gene activation through enhanced promoters, even if the essentiality of this histone mark to transcription start is still under debate [86,87]. While it would be odd to suggest that transcriptional activation via H3K4me3 is increased during hibernation, as this appears to counter the philosophy of MRD, H3K4 methylation is linked to transcriptional suppression via Notch signaling, which was examined earlier in this discussion. It is possible that H3K4 methylation is directly linked to the RBP-J repressor complex and therefore activates Notch to assist in suppressing gene expression [58]. Further investigation is needed to elucidate the precise histone modifications being enacted during hibernation, and their

resulting functional roles.

Histone modifications and their role during hibernation have been the subject of only preliminary studies. For example, in *I. tridecemlineatus* white adipose tissue, there is a strong reduction of "permissive" histone marks while the more metabolically active brown adipose tissue showed an increase in permissive histone marks, perhaps indicating differing requirements for gene transcription during hibernation [88,89]. Meanwhile, in both liver and muscle tissues of *I. tridecemlineatus*, an increase in permissive H3K4me1 was observed during torpor entry and during interbout arousals, indicating the existence of protective mechanisms in both tissues [90]. Further examination of histone modifications in euthermic vs. torpid skeletal muscle of *I. tridecemlineatus* revealed lysine 19 and 24 acetylation in histone H3, and lysine 6, 47, 110, and 117 acetylation in histone H2B [12]. Transcriptomic data in *M. auratus* suggested decreased RNA transcription in liver during torpor [71], accompanied by a potentially-related upregulation of SETDB1, SCL25A18, and ACADVL transcripts in *D. gliroides* liver [72]. SETDB1 is a histone methyltransferase often linked with transcriptional repression [83,84,12], which corroborates the GO terms in *E. quercinus* involving histone H3K4 trimethylation, histone exchange, chromatin silencing, and histone binding along with the corresponding terms for decreased RNA transcription (Figs. 2 and 3). Overall, histone modifications are species- and tissue-specific, further reinforcing the need for additional studies to quantify the precise histone modifications during hibernation in *E. quercinus* liver.

5. Conclusions

Overall, miRNA influence during hibernation seems to center around three main "themes": a switch in energy metabolism towards fatty acid oxidation; histone and chromatin modifications; and DNA replication/cell cycle. Many terms support the overarching theme of MRD during hibernation, with an interesting possibility of transcriptional suppression via Notch and its interaction with H3K4 methylation. Further research must be conducted to elucidate the exact roles of histone modifications during hibernation, and to validate the potential of Notch signaling and its functional outcomes. Finally, experimental validation would be prudent to isolate the exact number of miRNAs which are differentially-regulated during hibernation and whether FDR-adjustment may be interfering with the true number of miRNAs which change during hibernation in *E. quercinus*, especially given only 4 biological replicates per season were analyzed. This study offers broad areas of investigation to pursue hibernation-responsive biological changes in liver tissue, and provides the first study using next-generation sequencing to predict miRNA involvement in *E. quercinus* during hibernation.

CRediT authorship contribution statement

W. Aline Ingelson-Filpula: Writing – original draft, Visualization, Methodology, Formal analysis, Conceptualization. **Anna Kübber-Heiss:** Resources, Methodology. **Johanna Painer:** Resources, Methodology. **Gabrielle Stalder:** Resources, Methodology. **Hanane Hadj-Moussa:** Writing – review & editing, Methodology, Data curation, Conceptualization. **Fabrice Bertile:** Writing – review & editing, Resources, Methodology. **Caroline Habold:** Writing – review & editing, Resources, Methodology. **Sylvain Giroud:** Writing – review & editing, Resources, Project administration, Investigation, Funding acquisition, Data curation, Conceptualization. **Kenneth B. Storey:** Writing – review & editing, Supervision, Resources, Project administration, Conceptualization.

Ethics statement

All procedures regarding dormice experiments were approved by the Ethics and Animal Welfare Committee of the University of Veterinary Medicine Vienna in accordance with the University's guidelines for Good Scientific Practice and authorized by the Austrian Federal Ministry of Education, Science and Research (BMBWF-68.205/0137-WF/V/3b/2014) in accordance with current legislation.

Availability of supporting data

The genome files for *E. quercinus* have been uploaded to the SRA database (SRA Accession: PRJNA955229). All supplementary data has been uploaded with the manuscript.

Funding

This work was supported by the Austrian Science Fund (FWF; P 27267 and P 31577 to S.G.) and the city of Vienna. K.B.S. holds a discovery grant from the Natural Science and Engineering Research Council of Canada (RGPIN-2020-04733). An Ontario Graduate Scholarship is held by A.I.F. K.B.S. also holds the Canada Research Chair in Molecular Physiology.

Declaration of competing interest

The authors declare no conflict of interest.

Appendix A. Supplementary data

Supplementary data to this article can be found online at https://doi.org/10.1016/j.cryobiol.2024.105191.

References

[1] H.V. Carey, M.T. Andrews, S.L. Martin, Mammalian hibernation: cellular and molecular responses to depressed metabolism and low temperature, Physiol. Rev. 83 (2003) 1153–1181.
[2] S. Giroud, C. Habold, R.F. Nespolo, C. Mejías, J. Terrien, S.M. Logan, R.H. Henning, K.B. Storey, The torpid state: recent advances in metabolic adaptations and protective mechanisms, Front. Physiol. 11 (2021) 1824.
[3] T. Ruf, F. Geiser, Daily torpor and hibernation in birds and mammals, Biol. Rev. Camb. Phil. Soc. 90 (2015) 891–926.
[4] T. Ruf, K. Gasch, G. Stalder, H. Gerritsmann, S. Giroud, An hourglass mechanism controls torpor bout length in hibernating garden dormice, J. Exp. Biol. 224 (2021).
[5] K.B. Storey, J.M. Storey, Metabolic rate depression. The biochemistry of mammalian hibernation, in: G. Makowski (Ed.), Adv Clin Chem, Academic Press, Burlington, 2010, pp. 77–78.
[6] B. Mahlert, H. Gerritsmann, G. Stalder, T. Ruf, A. Zahariev, S. Blanc, S. Giroud, Implications of being born late in the active season for growth, fattening, torpor use, winter survival and fecundity, Elife 7 (2018).
[7] K.B. Storey, J.M. Storey, Metabolic rate depression and biochemical adaptation in anaerobiosis, hibernation and estivation, QRB (Q. Rev. Biol.) (1990).
[8] W.A. Ingelson-Filpula, K.B. Storey, Muscles in winter: the epigenetics of metabolic arrest, Epigenomes 5 (2021).
[9] K.B. Storey, Regulation of hypometabolism: insights into epigenetic controls, J. Exp. Biol. 218 (2015) 150–159.
[10] D. Lang-Ouellette, P.J. Morin, Differential expression of miRNAs with metabolic implications in hibernating thirteen-lined ground squirrels, *Ictidomys tridecemlineatus*, Mol. Cell. Biochem. 394 (2014) 291–298.
[11] Y. Liu, W. Hu, H. Wang, M. Lu, C. Shao, C. Menzel, Z. Yan, Y. Li, S. Zhao, P. Khaitovich, M. Liu, W. Chen, B.M. Barnes, J. Yan, Genomic analysis of miRNAs in an extreme mammalian hibernator, the Arctic ground squirrel, Physiol. Genom. 42A (2010) 39–51.
[12] S.N. Tessier, B.E. Luu, J.C. Smith, K.B. Storey, The role of global histone post-translational modifications during mammalian hibernation, Cryobiology 75 (2017) 28–36.
[13] D.P. Bartel, MicroRNAs: genomics, biogenesis, mechanism, and function, Cell 116 (2004) 281–297.
[14] S.M. Logan, K.B. Storey, MicroRNA expression patterns in the brown fat of hibernating 13-lined ground squirrels, Genomics 113 (2021) 769–781.
[15] B.E. Luu, E. Lefai, S. Giroud, J.E. Swenson, B. Chazarin, G. Gauquelin-Koch, J. M. Arnemo, A.L. Evans, F. Bertile, K.B. Storey, MicroRNAs facilitate skeletal muscle maintenance and metabolic suppression in hibernating brown bears, J. Cell. Physiol. 235 (2020) 3984–3993.
[16] M.D. Morin, D. Lang-Ouellette, P.J. Lyons, N. Crapoulet, P. Morin, Characterization of miRNAs modulated by torpor in the hibernating ground squirrel *Ictidomys tridecemlineatus* liver by next-generation sequencing, Cryo Lett. 38 (2017) 269–277.
[17] Y. Hu, W. Lan, D. Miller, Next-generation sequencing for MicroRNA expression profile, Methods Mol. Biol. 1617 (2017) 169–177.

[18] P. Liu, MicroRNA expression analysis: next-generation sequencing, Methods Mol. Biol. 1783 (2018) 171–183.
[19] J. Zhang, K.B. Storey, RBiomirGS: an all-in-one miRNA gene set analysis solution featuring target mRNA mapping and expression profile integration, PeerJ 2018 (2018) 1–17.
[20] A.G. Hindle, K.R. Grabek, L. Elaine Epperson, A. Karimpour-Fard, S.L. Martin, Metabolic changes associated with the long winter fast dominate the liver proteome in 13-lined ground squirrels, Physiol. Genom. 46 (2014) 348–361.
[21] C.C. Kurtz, J.P. Otis, M.D. Regan, H.V. Carey, How the gut and liver hibernate, Comp. Biochem. Physiol. Mol. Integr. Physiol. 253 (2021) 110875.
[22] S. Giroud, S. Zahn, F. Criscuolo, I. Chery, S. Blanc, C. Turbill, T. Ruf, Late-born intermittently fasted juvenile garden dormice use torpor to grow and fatten prior to hibernation: consequences for ageing processes, Proc. Biol. Sci. 281 (2014).
[23] N. Huber, S. Vetter, G. Stalder, H. Gerritsmann, S. Giroud, Dynamic function and composition shift in circulating innate immune cells in hibernating garden dormice, Front. Physiol. 12 (2021).
[24] S. Giroud, G. Stalder, H. Gerritsmann, A. Kübber-Heiss, J. Kwak, W. Arnold, T. Ruf, Dietary lipids affect the onset of hibernation in the garden dormouse (eliomys quercinus): implications for cardiac function, Front. Physiol. 9 (2018).
[25] H. Hadj-Moussa, M.E. Pamenter, K.B. Storey, Hypoxic naked mole-rat brains use microRNA to coordinate hypometabolic fuels and neuroprotective defenses, J. Cell. Physiol. 236 (2021) 5080–5097.
[26] J. Zhang, H. Hadj-Moussa, K.B. Storey, Current progress of high-throughput microRNA differential expression analysis and random forest gene selection for model and non-model systems: an R implementation, J Integr Bioinform (2016).
[27] M. Martin, Cutadapt removes adapter sequences from high-throughput sequencing reads. EMBnet J, 2011.
[28] S. Andrews, FASTQC A Quality Control Tool for High Throughput Sequence Data, Babraham Institute, 2015.
[29] I. Kalvari, J. Argasinska, N. Quinones-Olvera, E.P. Nawrocki, E. Rivas, S.R. Eddy, A. Bateman, R.D. Finn, A.I. Petrov, Rfam 13.0: shifting to a genome-centric resource for non-coding RNA families, Nucleic Acids Res. (2018).
[30] S. Sai lakshmi, S. Agrawal, piRNABank: a web resource on classified and clustered Piwi-interacting RNAs, Nucleic Acids Res. (2008).
[31] B. Langmead, C. Trapnell, M. Pop, S.L. Salzberg, Ultrafast and memory-efficient alignment of short DNA sequences to the human genome, Genome Biol. (2009).
[32] A. Kozomara, M. Birgaoanu, S. Griffiths-Jones, MiRBase: from microRNA sequences to function, Nucleic Acids Res. 47 (2019) D155–D162.
[33] H. Li, B. Handsaker, A. Wysoker, T. Fennell, J. Ruan, N. Homer, G. Marth, G. Abecasis, R. Durbin, The sequence alignment/map format and SAMtools, Bioinformatics 25 (2009) 2078–2079.
[34] C.W. Law, Y. Chen, W. Shi, G.K. Smyth, Voom: precision weights unlock linear model analysis tools for RNA-seq read counts, Genome Biol. (2014).
[35] M.E. Ritchie, B. Phipson, D. Wu, Y. Hu, C.W. Law, W. Shi, G.K. Smyth, Limma powers differential expression analyses for RNA-sequencing and microarray studies, Nucleic Acids Res. (2015).
[36] J.D. Storey, The Positive False Discovery Rate: a Bayesian Interpretation and the Q-Value, 2003, pp. 2013–2035.
[37] T. Tong, H. Zhao, Practical guidelines for assessing power and false discovery rate for a fixed sample size in microarray experiments, Stat. Med. 27 (2008) 1960.
[38] S. Carbon, E. Douglass, N. Dunn, B. Good, N.L. Harris, S.E. Lewis, C.J. Mungall, S. Basu, R.L. Chisholm, R.J. Dodson, E. Hartline, P. Fey, P.D. Thomas, L.P. Albou, D. Ebert, M.J. Kesling, H. Mi, A. Muruganujan, X. Huang, S. Poudel, T. Mushayahama, J.C. Hu, S.A. LaBonte, D.A. Siegele, G. Antonazzo, H. Attrill, N. H. Brown, S. Fexova, P. Garapati, T.E.M. Jones, S.J. Marygold, G.H. Millburn, A. J. Rey, V. Trovisco, G. Dos Santos, D.B. Emmert, K. Falls, P. Zhou, J.L. Goodman, V. B. Strelets, J. Thurmond, M. Courtot, D.S. Osumi, H. Parkinson, P. Roncaglia, M. L. Acencio, M. Kuiper, A. Lreid, C. Logie, R.C. Lovering, R.P. Huntley, P. Denny, N. H. Campbell, B. Kramarz, V. Acquaah, S.H. Ahmad, H. Chen, J.H. Rawson, M. C. Chibucos, M. Giglio, S. Nadendla, R. Tauber, M.J. Duesbury, N.T. Del, B.H. M. Meldal, L. Perfetto, P. Porras, S. Orchard, A. Shrivastava, Z. Xie, H.Y. Chang, R. D. Finn, A.L. Mitchell, N.D. Rawlings, L. Richardson, A. Sangrador-Vegas, J. A. Blake, K.R. Christie, M.E. Dolan, H.J. Drabkin, D.P. Hill, L. Ni, D. Sitnikov, M. A. Harris, S.G. Oliver, K. Rutherford, V. Wood, J. Hayles, J. Bahler, A. Lock, E. R. Bolton, J. De Pons, M. Dwinell, G.T. Hayman, S.J.F. Laulederkind, M. Shimoyama, M. Tutaj, S.J. Wang, P. D'Eustachio, L. Matthews, J.P. Balhoff, S. A. Aleksander, G. Binkley, B.L. Dunn, J.M. Cherry, S.R. Engel, F. Gondwe, K. Karra, K.A. MacPherson, S.R. Miyasato, R.S. Nash, P.C. Ng, T.K. Sheppard, A. Shrivatsav Vp, M. Simison, M.S. Skrzypek, S. Weng, E.D. Wong, M. Feuermann, P. Gaudet, E. Bakker, T.Z. Berardini, L. Reiser, S. Subramaniam, E. Huala, C. Arighi, A. Auchincloss, K. Axelsen, G.P. Argoud, A. Bateman, B. Bely, M.C. Blatter, E. Boutet, L. Breuza, A. Bridge, R. Britto, H. Bye-A-Jee, C. Casals-Casas, E. Coudert, A. Estreicher, L. Famiglietti, P. Garmiri, G. Georghiou, A. Gos, N. Gruaz-Gumowski, E. Hatton-Ellis, U. Hinz, C. Hulo, A. Ignatchenko, F. Jungo, G. Keller, K. Laiho, P. Lemercier, D. Lieberherr, Y. Lussi, A. Mac-Dougall, M. Magrane, M.J. Martin, P. Masson, D.A. Natale, N.N. Hyka, I. Pedruzzi, K. Pichler, S. Poux, C. Rivoire, M. Rodriguez-Lopez, T. Sawford, E. Speretta, A. Shypitsyna, A. Stutz, S. Sundaram, M. Tognolli, N. Tyagi, K. Warner, R. Zaru, C. Wu, J. Chan, J. Cho, S. Gao, C. Grove, M.C. Harrison, K. Howe, R. Lee, J. Mendel, H.M. Muller, D. Raciti, K. Van Auken, M. Berriman, L. Stein, P.W. Sternberg, D. Howe, S. Toro, M. Westerfield, The gene ontology resource: 20 years and still GOing strong, Nucleic Acids Res. 47 (2019) D330–D338.
[39] M. Kanehisa, Y. Sato, M. Furumichi, K. Morishima, M. Tanabe, New approach for understanding genome variations in KEGG, Nucleic Acids Res. (2019).
[40] F. Garcia-Garcia, J. Panadero, J. Dopazo, D. Montaner, Integrated gene set analysis for microRNA studies, Bioinformatics (2016).
[41] D. Karagkouni, M.D. Paraskevopoulou, S. Chatzopoulos, I.S. Vlachos, S. Tastsoglou, I. Kanellos, D. Papadimitriou, I. Kavakiotis, S. Maniou, G. Skoufos, T. Vergoulis, T. Dalamagas, A.G. Hatzigeorgiou, DIANA-TarBase v8: a decade-long collection of experimentally supported miRNA-gene interactions, Nucleic Acids Res. 46 (2018) D239–D245.
[42] A. Liberzon, C. Birger, H. Thorvaldsdóttir, M. Ghandi, J.P. Mesirov, P. Tamayo, The Molecular Signatures Database (MSigDB) hallmark gene set collection, Cell Syst 1 (2015) 417.
[43] H. Wickham, W. Chang, L. Henry, T.L. Pedersen, K. Takahashi, C. Wilke, K. Woo, H. Yutani, D. Dunnington, T. van den Brand, ggplot2: Create Elegant Data Visualisations Using the Grammar of Graphics, CRAN, 2007. Contributed Packages.
[44] E. Neuwirth, RColorBrewer: ColorBrewer Palettes, CRAN, 2002.
[45] H. Wickham, D. Vaughan, M. Girlich, Tidyr: Tidy Messy Data, CRAN, 2014.
[46] H. Wickham, R. François, L. Henry, K. Müller, D. Vaughan, Dplyr: A Grammar of Data Manipulation, CRAN, 2014.
[47] J.D. Hunter, Matplotlib: a 2D graphics environment, Comput. Sci. Eng. (2007).
[48] M. Waskom, O. Botvinnik, P. Hobson, J. Warmenhoven, J.B. Cole, Y. Halchenko, J. Vanderplas, S. Hoyer, S. Villalba, E. Quintero, A. Miles, Seaborn: Statistical Data Visualization, 2014.
[49] G.R. Warnes, B. Bolker, L. Bonebakker, R. Gentleman, W.H.A. Liaw, T. Lumley, M. Maechler, A. Magnusson, S. Moeller, M. Schwartz, B. Venables, Gplots: various R programming tools for plotting data, R package version 3.0.1.1 (2019).
[50] H. Wang, C. Zang, X.S. Liu, J.C. Aster, The role of Notch receptors in transcriptional regulation, J. Cell. Physiol. 230 (2015) 982.
[51] S.J. Bray, Notch signalling in context, Nat. Rev. Mol. Cell Biol. 17 (11 17) (2016) 722–735.
[52] Y. Sun, W.Z. Liu, T. Liu, X. Feng, N. Yang, H.F. Zhou, Signaling pathway of MAPK/ERK in cell proliferation, differentiation, migration, senescence and apoptosis, J. Recept. Signal Transduction 35 (2015) 600–604.
[53] C.L. Childers, S.N. Tessier, K.B. Storey, The heart of a hibernator: EGFR and MAPK signaling in cardiac muscle during the hibernation of thirteen-lined ground squirrels, Ictidomys tridecemlineatus, PeerJ 7 (2019).
[54] S.F. Eddy, K.B. Storey, p38 MAPK regulation of transcription factor targets in muscle and heart of the hibernating bat, Myotis lucifugus, Cell Biochem. Funct. 25 (2007) 759–765.
[55] A. Erman, L.J. Hawkins, K.B. Storey, Changes in microRNA expression related to ischemia-reperfusion injury in the kidney of the thirteen-lined ground squirrel during torpor, Biochimie 225 (2024) 40–48.
[56] W.A. Ingelson-Filpula, K.B. Storey, Hibernation-induced microRNA expression promotes signaling pathways and cell cycle dysregulation in ictidomys tridecemlineatus cardiac tissue, Metabolites 13 (2023).
[57] C.W. Wu, K.B. Storey, Pattern of cellular quiescence over the hibernation cycle in liver of thirteen-lined ground squirrels, Cell Cycle 11 (2012) 1714–1726.
[58] R. Liefke, F. Oswald, C. Alvarado, D. Ferres-Marco, G. Mittler, P. Rodriguez, M. Dominguez, T. Borggrefe, Histone demethylase KDM5A is an integral part of the core Notch-RBP-J repressor complex, Genes Dev. 24 (2010) 590–601.
[59] M. ming Ni, Y. rui Wang, W. wen Wu, C. cai Xia, Y. he Zhang, J. Xu, T. Xu, J. Li, Novel Insights on Notch signaling pathways in liver fibrosis, Eur. J. Pharmacol. 826 (2018) 66–74.
[60] Y. Wang, F. Zhou, M. Li, Y. Zhang, N. Li, L. Shao, MiR-34a-5p promotes hepatic gluconeogenesis by suppressing SIRT1 expression, Exp. Cell Res. 420 (2022).
[61] L.E. Epperson, T.A. Dahl, S.L. Martin, Quantitative analysis of liver protein expression during hibernation in the golden-mantled ground squirrel, Mol. Cell. Proteomics 3 (2004) 920–933.
[62] S.C. Gehnrich, J.R. Aprille, Hepatic gluconeogenesis and mitochondrial function during hibernation, Comp. Biochem. Physiol. B 91 (1988) 11–16.
[63] C.T. Williams, A.V. Goropashnaya, C.L. Buck, V.B. Fedorov, F. Kohl, T.N. Lee, B. M. Barnes, Hibernating above the permafrost: effects of ambient temperature and season on expression of metabolic genes in liver and brown adipose tissue of arctic ground squirrels, J. Exp. Biol. 214 (2011) 1300–1306.
[64] C.W. Wu, K.K. Biggar, K.B. Storey, Biochemical adaptations of mammalian hibernation: exploring squirrels as a perspective model for naturally induced reversible insulin resistance, Braz. J. Med. Biol. Res. 46 (2013) 1–13.
[65] B.E. Luu, K.K. Biggar, C.W. Wu, K.B. Storey, Torpor-responsive expression of novel microRNA regulating metabolism and other cellular pathways in the thirteen-lined ground squirrel, Ictidomys tridecemlineatus, FEBS Lett. 590 (2016) 3574–3582.
[66] M. Hampton, R.G. Melvin, A.H. Kendall, B.R. Kirkpatrick, N. Peterson, M. T. Andrews, Deep sequencing the transcriptome reveals seasonal adaptive mechanisms in a hibernating mammal, PLoS One 6 (2011).
[67] B.L. Krilowicz, Ketone body metabolism in a ground squirrel during hibernation and fasting, Am. J. Physiol. 249 (1985).
[68] L.C. Mokrasch, H.J. Grady, S. Grisolia, Thermogenic and adaptive mechanisms in hibernation and arousal from hibernation, Am. J. Physiol. 199 (1960) 945–949.
[69] J.C. Rauch, H.W. Behrisch, J.C. Rauch, H.W. Behrisch, Ketone bodies: a source of energy during hibernation 59 (2011) 754–760.
[70] L.S. Tashima, S.J. Adelstein, C.P. Lyman, Radioglucose utilization by active, hibernating, and arousing ground squirrels, Am. J. Physiol. 218 (1970) 303–309.
[71] L. Coussement, M.M. Oosterhof, V. Guryev, V.A. Reitsema, J.J. Bruintjes, M. Goris, H.R. Bouma, T. De Meyer, M.G. Rots, R.H. Henning, Liver transcriptomic and methylomic analyses identify transcriptional mitogen-activated protein kinase regulation in facultative hibernation of Syrian hamster, Proceedings of the Royal Society B 290 (2023).
[72] R.F. Nespolo, J.D. Gaitan-Espitia, J.F. Quintero-Galvis, F.V. Fernandez, A.X. Silva, C. Molina, K.B. Storey, F. Bozinovic, A functional transcriptomic analysis in the relict marsupial Dromiciops gliroides reveals adaptive regulation of protective functions during hibernation, Mol. Ecol. 27 (2018) 4489–4500.

[73] L.E. Hand, B.R.C. Saer, S.T. Hui, H.A. Jinnah, S. Steinlechner, A.S.I. Loudon, D. A. Bechtold, Induction of the metabolic regulator Txnip in fasting-induced and natural torpor, Endocrinology 154 (2013) 2081–2091.
[74] L.K. Bogren, K.R. Grabek, G.S. Barsh, S.L. Martin, Comparative tissue transcriptomics highlights dynamic differences among tissues but conserved metabolic transcript prioritization in preparation for arousal from torpor, J. Comp. Physiol. B 187 (2017) 735–748.
[75] K.B. Storey, Hypometabolism and the cell cycle, Cell Cycle 11 (2012) 1665.
[76] M. Sokolović, D. Wehkamp, A. Sokolović, J. Vermeulen, L.A. Gilhuijs-Pederson, R. I.M. van Haaften, Y. Nikolsky, C.T.A. Evelo, A.H.C. van Kampen, T.B.M. Hakvoort, W.H. Lamers, Fasting induces a biphasic adaptive metabolic response in murine small intestine, BMC Genom. 8 (2007).
[77] K.B. Storey, J.M. Storey, Metabolic rate depression in animals: transcriptional and translational controls, Biol. Rev. Camb. Phil. Soc. 79 (2004) 207–233.
[78] G. Singh, T. Bloskie, K.B. Storey, Tissue-specific response of the RB-E2F1 complex during mammalian hibernation, J Exp Zool A Ecol Integr Physiol 337 (2022) 1002–1009.
[79] T.B. Kheir, A.H. Lund, Epigenetic dynamics across the cell cycle, Essays Biochem. 48 (2010) 107–120.
[80] I. Rabinovich-Nikitin, R. Dhingra, L.A. Kirshenbaum, Epigenetic regulation of cardiac cell cycle Re-entry and proliferation, J. Mol. Cell. Cardiol. 121 (2018) 297–299.
[81] S.N. Tessier, W.A. Ingelson-Filpula, K.B. Storey, Epigenetic regulation by DNA methyltransferases during torpor in the thirteen-lined ground squirrel *Ictidomys tridecemlineatus*, Mol. Cell. Biochem. 476 (2021) 3975–3985.
[82] D. Tsukamoto, M. Ito, N. Takamatsu, Epigenetic regulation of hibernation-associated HP-20 and HP-27 gene transcription in chipmunk liver, Biochem. Biophys. Res. Commun. 495 (2018) 1758–1765.
[83] M. Grunstein, Histone acetylation in chromatin structure and transcription, Nature 389 (1997) 349–352.
[84] K. Hyun, J. Jeon, K. Park, J. Kim, Writing, erasing and reading histone lysine methylations, Exp. Mol. Med. 49 (2017) e324.
[85] T. Kouzarides, Chromatin modifications and their function, Cell 128 (2007) 693–705.
[86] T.H. Beacon, G.P. Delcuve, C. López, G. Nardocci, I. Kovalchuk, A.J. van Wijnen, J. R. Davie, The dynamic broad epigenetic (H3K4me3, H3K27ac) domain as a mark of essential genes, Clin. Epigenet. 13 (2021).
[87] F.S. Howe, H. Fischl, S.C. Murray, J. Mellor, Is H3K4me3 instructive for transcription activation? Bioessays 39 (2017) 1–12.
[88] A.N. Rouble, L.J. Hawkins, K.B. Storey, Roles for lysine acetyltransferases during mammalian hibernation, J. Therm. Biol. (2018).
[89] A.N. Rouble, K.B. Storey, Characterization of the SIRT family of NAD+-dependent protein deacetylases in the context of a mammalian model of hibernation, the thirteen-lined ground squirrel, Cryobiology 71 (2015) 334–343.
[90] A.J. Watts, K.B. Storey, Hibernation impacts lysine methylation dynamics in the 13-lined ground squirrel, *Ictidomys tridecemlineatus*, J Exp Zool A Ecol Integr Physiol 331 (2019) 234–244.